Robust 2D Diffusion Weighted Chemical Shift Imaging (DW-CSI) of the human brain at 7T

Ece Ercan[1], Aranee Techawiboonwong[2], Maarten J. Versluis[1], Andrew G. Webb[1], and Itamar Ronen[1]

[1]C.J. Gorter Center for High Field MRI, Department of Radiology, Leiden University Medical Center, Leiden, Netherlands, [2]Electrical Engineering, Mahidol University, Nakornpathom, Thailand

Purpose: Diffusion weighted spectroscopy (DWS) probes the diffusion properties of intracellular metabolites such as N-acetyl aspartate (NAA), creatine (tCr) and choline (tCho), and is thus a unique tool for compartment-specific assessment of tissue microstructure [1]. Single-volume (SV) DWS has been shown to yield meaningful and reproducible results in humans[1-4], however only a few attempts have been made so far to obtain DWS images of brain metabolites with DW chemical shift imaging (CSI)[5-7]. The main challenge has been to obtain robust and reproducible DWS maps. The multi-shot nature of the acquisition, combined with the low signal-to-noise ratio and the relatively high gradient strength needed for adequate diffusion weighting of the slow diffusing metabolites, all contribute to strong inter-shot phase and amplitude fluctuations that strongly affect the resulting DW spectra. Here, we show for the first time a method that accounts for both amplitude and phase inter-shot fluctuations, and generates robust, reproducible and anatomically meaningful DW-CSI and metabolite apparent diffusion coefficient (ADC) maps. The method presented here uses a real-time, navigator-based scheme which allows instantaneous re-acquisition of any corrupted diffusion-weighted k-space lines, as well as post-processing correction of gradient-induced phase fluctuations. We present test-retest results that confirm the robustness of the DW-CSI maps, and show meaningful correlation between the ADC of NAA and the voxel-wise tissue composition.

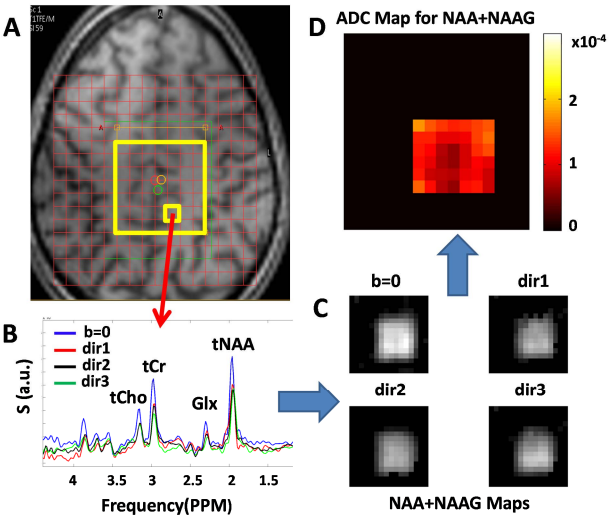

Fig.1. (A) Planning of the 2D DW-CSI experiment with VOI shown in yellow. **(B)** Spectra obtained from a single voxel of the VOI for b=0 and b= 2870 from 3 diffusion gradient directions **(C)** NAA+NAAG maps obtained for each separate condition **(D)** ADC map for NAA+NAAG obtained from one subject.

Methods: Experiments were performed on a 7 Tesla Achieva Philips MRI scanner equipped with a 32-channel receive coil array. Data acquired from 5 healthy volunteers (28.6±1.5 years, 1 female, 4 males) consist of 3D T_1-weighted images (0.85x0.85x1.00mm^3, TR/TE=4.94/2.17ms), Diffusion Tensor Images (2x2x2mm^3, TR/TE= 10,000/66 ms, one b=0 image and 15 encoding directions with a b-value of 1000 s/mm^2) and 2D DW-CSI data from a supra-callosal axial slice (Fig.1A) obtained with a Point Resolved Spectroscopy (PRESS) sequence with bipolar diffusion weighting gradients (FOV=96x96mm^2, matrix size=12x12, VOI=48x42x8mm^3, voxel size=6x6x8mm^3, TR/TE: 3 cardiac cycles (~3000ms)/100ms, turbo spectroscopic imaging (TSI) factor=2, readout BW=5kHz, 256 sample points, diffusion gradients applied in 3 orthogonal directions with δ= 34ms , Δ= 50ms , b-values of 0 and 2870 s/mm^2, total scan time 15-20 minutes). One of the subjects was scanned twice in order to evaluate the robustness of the method with a test-retest comparison. Water suppression with variable Pulse power and Optimized Relaxation Delays (VAPOR)[8] was de-optimized for the diffusion acquisitions to acquire sufficient water signal for eddy current correction. For each k-space location, a navigator (~30 data points prior to phase-encoding) was acquired. The amplitude of the navigator of the first few acquisitions at each DW condition was used to set a threshold for the subsequent spectral acquisitions, and data that fell below that threshold were reacquired.

Data Analysis: Gray matter (GM) and white matter (WM) tissue probabilities were calculated with FSL FAST software based on the T_1-weighted image. The average tissue fractions were calculated for each CSI voxel within the VOI with in-house developed MATLAB® code. DW-CSI data were also analyzed with in house developed MATLAB® routines in which the eddy current and diffusion related phase fluctuations are corrected. Spectral analysis was performed with LCModel and the results were read into a MATLAB code where the DW maps for each condition and the ADC map were calculated for each metabolite of interest. The process is illustrated in Figure 1.

Results and discussion: Figure 2 shows a test-retest comparison of the tNAA signal obtained from two consecutive DW-CSI acquisitions from the same subject indicates high reproducibility (R^2=0.96, 0.95, 0.87 and 0.96 for b0, d1, d2 and d3, respectively) of the method. Corroboration of localization of the signal is given in Figure 3, where the ADC of tNAA is well correlated with WM fraction, in accordance with previous findings in single volume DWS[3]. Table 1 shows metabolite ADC values for white and gray matter calculated and averaged over all subjects, and the ADC values compare well with SV DWS results obtained previously[2-4].

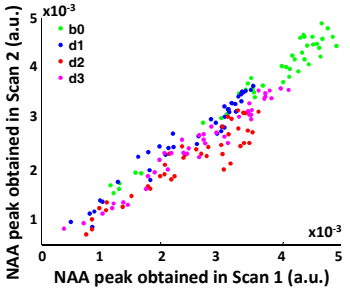

Fig.2 Comparison of test re-test values.

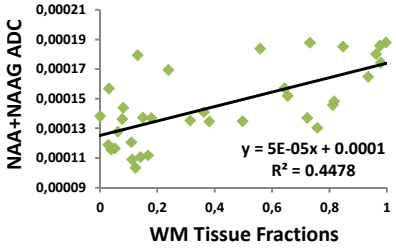

Fig.3 Correlation of WM tissue fractions of each VOI voxel with NAA+NAAG ADC values in mm^2/s.

Table1. ADC of different metabolites calculated for GM and WM.

Metabolite	WM ADC (10^{-3} mm^2/s)	GM ADC (10^{-3} mm^2/s)
NAA	1.47± 0.39	1.00±0.41
Creatine	1.28±0.42	1.45±0.43
Choline	1.15±0.25	0.90±0.45

Conclusion: We have introduced a robust and reproducible implementation of DW-CSI. The reproducibility of the DWS metabolite maps, as well as the mapping of the NAA ADC to WM tissue fraction, and reliable metabolite ADC values show that DW-CSI is a promising method for mapping compartment-specific microstructural properties in the brain. **References: 1.** Nikolay, K. et al., NMR Biomed (2001) **2.** Ellegood, J., et al., MRM (2006) **3.** Wood, E.T., et al. J Neuroscience (2012) **3.** Kan, H., et al. MRM (2012) **4.** Ronen, I., et al., Brain Struct Funct (2013) **5.** Ronen I. et al. Proc. ISMRM 2008 **6.** Techawiboonwong, A., et al. Proc. ISMRM 2011 **7.** Posse, S., et al., Proc. ISMRM 2013 **8.** Tkac, I., et al., MRM (1999).